

Research Article

Optimization of Ferrite Number of Solution Annealed Duplex Stainless Steel Cladding Using Integrated Artificial Neural Network: Simulated Annealing

¹V. Rathinam and ²T. Kannan

¹Department of Automobile Engineering, Paavaai Group of Institutions,
Namakkal 637018, Tamilnadu, India

²S.V.S. College of Engineering, Coimbatore 642109, Tamilnadu, India

Abstract: Cladding is the most economical process used on the surface of low carbon structural steel to improve the corrosion resistance. The corrosion resistant property is based on the amount of ferrite present in the clad layer. Generally, the ferrite content present in the layer is expressed in terms of Ferrite Number (FN). The optimum range of ferrite number provides adequate surface properties like chloride stress corrosion cracking resistance, pitting and crevice corrosion resistance and mechanical properties. For achieving maximum economy and enhanced life, duplex stainless steel (E2209T1-4/1) is deposited on the surface of low carbon structural steel of IS: 2062. The problem faced in the weld cladding towards achieving the required amount of ferrite number is selection of optimum combination of input process parameters. This study concentrates on estimating FN and analysis of input process parameters on FN of heat treated duplex stainless steel cladding. To predict FN, mathematical equations were developed based on four factor five level central composite rotatable design with full replication using regression methods. Then, the developed models were embedded further into integrated ANN-SA to estimate FN. From the results, the integrated ANN-SA is capable of giving maximum FN at optimum process parameters compared to that of experimental, regression and ANN modeling.

Keywords: Artificial neural network, duplex stainless steel, ferrite number, flux cored arc welding, simulated annealing, solution annealing heat treatment

INTRODUCTION

Today, both utilization of engineering materials and its availability are inversely proportional due to diminishing of natural resources. Hence, implementing innovative method is absolutely necessary in the field of fabrication industry. Apart from this, industries such as paper, chemical, fertilizer, nuclear, food processing, petrochemical and other allied industries require their components with special surface properties such as stress corrosion cracking, pitting and crevice corrosion resistance, wear resistance and hardness etc. So, the most effective and economical method of producing a thick layer on the surface of low carbon steel is cladding process. It consist of following advantages:

- The fusion bonding of the material with the substrate is good.
- It is easy to use and it consists of component that has improved surface properties.

Here, Duplex Stainless Steel (DSS) is used for surface cladding, where a high energy density source such as an electric arc has been widely used

commercially to enhance the surface properties of the materials. Various welding processes employed for cladding are Shielded Metal Arc Welding (SMAW), Gas Tungsten Arc Welding (GTAW), Submerged Arc Welding (SAW), Gas Metal Arc Welding (GMAW), Flux Cored Arc Welding (FCAW), Electroslag Welding (ESW), Oxyacetylene Welding (OAW) and Explosive welding (Murugan and Parmer, 1994). In FCAW process, an electric arc is used between a continuous supply of duplex stainless steel filler metal and the weld pool, with shielding from externally supplied gas which may be carbon dioxide to provide stable arc, uniform metal transfer. The heat of the arc melts the surface of base metal and end of the electrode. The molten metal from the electrode is transferred and deposited on the surface of the base metal. The characteristics of the weld metal are mainly depending on the presence of ferrite number, which is key factor to decide many desired properties. The presence of FN in duplex stainless steel clad metal plays a major role to determining mechanical and surface properties. Namely, properties of DSS clad metals such as corrosion, wear resistance are predicted by estimating FN. A minimum FN is necessary to avoid hot cracking

Corresponding Author: V. Rathinam, Department of Automobile Engineering, Paavaai Group of Institutions, Namakkal 637018, Tamilnadu, India

This work is licensed under a Creative Commons Attribution 4.0 International License (URL: <http://creativecommons.org/licenses/by/4.0/>).

whereas maximum FN determines the propensity to embrittlement due to second phase precipitation. Particularly, strength and stress corrosion cracking resistance may be reduced when FN is less than 30. Similarly, there is some loss in ductility and toughness, when the FN is above 70 (Kotecki, 1997). Hence, the clad weld structure was embedded into solution annealing heat treatment to increase FN with above said process parameters.

Experimental setup: The test specimens were cut from the base metal of low carbon structural steel (IS: 2062) plate with the size of 200×150×20 mm. Before cladding, the surface of the base metal was ground as per the metallurgical procedure for the purpose of removing oxide scale and dirt. The material used for cladding process is flux cored duplex stainless steel welding wire E2209T1-4/1 with the size of 1.2 mm diameter. The details of chemical compositions of filler and base metal are given in Table 1.

Schematic of cladded specimen: The FN and properties of clad metals are strongly influenced by dilution, which depends on input process parameters. Dilution is the ratio of the amount of Base metal melted (B) to the sum of the filler metal Added and Base metal melted (A+B). The geometrical characteristics of weld bead are shown in Fig. 1.

Experimental parameters and design: The cladding experiments were conducted on a constant voltage programmable welding machine (Unimacro 501C). The experimental setup used for this study is a travelling carriage with a table for supporting the specimen. The welding gun was held stationary in a frame mounted above the worktable and it consists of an arrangement with multidirectional positions. In this experiment, a stringer bead technique was used for laying the beads with constant overlap of 40% and the interpass temperature of 150°C was maintained during cladding experiment. The experimental setup is shown in Fig. 2. To protect the molten metal from atmospheric gases, carbon dioxide was used at the rate of 18 L/min with constant flow rate to maintain a stable arc and uniform metal transfer. The presence of FN in the duplex

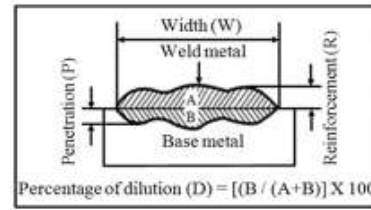


Fig. 1: Characteristics of weld bead geometry

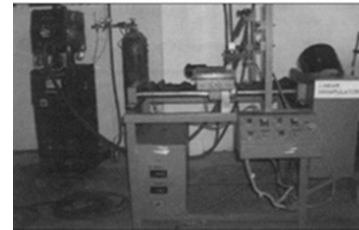


Fig. 2: Experimental setup for cladding

stainless steel clad metal is a vital role to obtain the required properties. FN in the clad weld metal by FCAW process is always affected by primary parameters viz welding current, welding speed and the secondary process parameters viz contact tip-to-specimen distance and gun angle. The working ranges of all selected parameters were fixed by conducting trial runs. This was carried out by varying one of the factors while keeping the rest of them at constant value. The working range of process parameters have been explored by inspection of bead appearance carried out by varying one of the factors while keeping the rest of them at constant value. The working range of process parameters have been explored by inspection of bead appearance without any visible defects such as surface porosity, undercut etc. In this regard, the FCAW process parameters and their levels with units are presented in Table 2. The upper limit of a factor was coded as +2 and the lower limit was coded as -2. The coded values for middle values can be calculated using the Eq. (1):

$$X_i = \frac{2[2X - (X_{max} + X_{min})]}{(X_{max} - X_{min})} \quad (1)$$

Table 1: Chemical composition of filler and base metals

Material	C	Si	Mn	S	Al	Cr	Mo	Ni	N ₂	Cu
IS: 2062	0.150	0.160	0.870	0.016	0.031	-	-	-	-	-
E2209 T1-4/1	0.023	0.760	1.030	0.002	-	23.14	3.05	9.22	0.13	0.09

Table 2: Welding parameters and their levels

Parameter	Unit	Notations	Factor levels				
			-2	-1	0	1	2
Welding current	A	I	200	225	250	275	300
Welding speed	cm/min	S	20	30	40	50	60
Contact tip-to-specimen distance	mm	N	22	24	26	28	30
Gun angle	degree	T	70	75	80	85	90

Table 3: Design matrix with ferrite number (after heat treatment)

Design matrix					
Trial No.	I	S	N	T	Measured FN
01	-1	-1	-1	-1	40
02	+1	-1	-1	-1	27
03	-1	+1	-1	-1	37
04	+1	+1	-1	-1	28
05	-1	-1	+1	-1	39
06	+1	-1	+1	-1	37
07	-1	+1	+1	-1	39
08	+1	+1	+1	-1	28
09	-1	-1	-1	+1	39
10	+1	-1	-1	+1	32
11	-1	+1	-1	+1	23
12	+1	+1	-1	+1	19
13	-1	-1	+1	+1	42
14	+1	-1	+1	+1	35
15	-1	+1	+1	+1	24
16	+1	+1	+1	+1	24
17	-2	0	0	0	49
18	+2	0	0	0	27
19	0	-2	0	0	38
20	0	+2	0	0	19
21	0	0	-2	0	33
22	0	0	+2	0	40
23	0	0	0	-2	36
24	0	0	0	+2	25
25	0	0	0	0	34
26	0	0	0	0	31
27	0	0	0	0	34
28	0	0	0	0	34
29	0	0	0	0	32
30	0	0	0	0	37
31	0	0	0	0	37



Fig. 3: Pit furnace used for the heat treatment of clad specimen

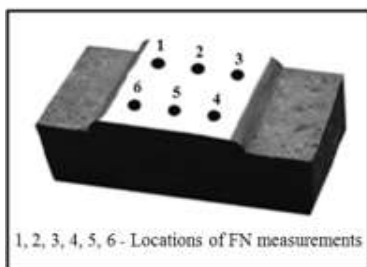


Fig. 4: Locations of FN measurements

where, X_i is the required coded value of parameter X , X is any value of a parameter from X_{\max} to X_{\min} , X_{\min} is the lower limit of the variable and X_{\max} is the upper limit of the parameter. Due to wide range of parameters a central composite rotatable design (Cochran and Cox, 1987) with full factorial was used. The experimental design has 31 runs that are shown in Table 3. This

design matrix consists of 16 rows ($2^4 = 16$) with full factorial and next eight rows show the star points and last seven rows show the star points and last seven rows exhibit the center point. The clad specimens were heat treated to increase the ferrite content and restore the ferrite and austenite phase balance. As the temperature is decreased, the amount of austenite increases whereas the amount of ferrite decreased. The unbalanced microstructure of the clad weld metal is altered by proper annealing heat treatment. Heat treatment at low temperature range (300° - 1000° C) will lead to form different phase precipitation (Karlsson *et al.*, 1995; Karlsson, 1999). In practical, many papers have paid more attention to reduce the FN when both filler and base metal were welded in DSS. The FN was increased, when increasing the heat treatment temperature (Lai *et al.*, 1995) and high aging temperature above 1000° C is also encouraged to increase the FN (Badji *et al.*, 2004, 2008) with changes in mechanical properties. Consequently, these treatments favor to minimize the undesirable precipitations at high temperature range. From previous research (Heejoon and Yongsoo, 2009) high temperature annealing treatment favors to increase the FN along with grain size. From previous research the test specimens were heat treated at constant temperature of 1093° C (Kotecki, 1989) and held the specimen at 1038° C for 4 h. The furnace used for heat treatment is pit furnace, which is shown in Fig. 3. To measure the FN in the heat treated specimen conveniently, the top surface of the clad specimens were ground towards longitudinal direction. The quantitative measurement of ferrite number was performed by magnetic measurement using the device, which is called Feritescope. These values are given in Table 3. To get optimum readings, the FN was measured as shown in Fig. 4, at six different points from three consecutive beads towards longitudinal axis. The device used for measuring the FN was calibrated in accordance with procedures specified in ANSI/AWS A 4.2.

METHODOLOGY

The following modules are involved in this study. These are:

- Experimental data
- Regression modeling
- ANN modeling
- Optimization of SA
- Integrated ANN-SA type A
- Integrated ANN-SA type B

The objectives of two integrated systems are:

- To estimate the maximum FN of Solution annealed duplex stainless steel cladding is compared with regression and ANN models.

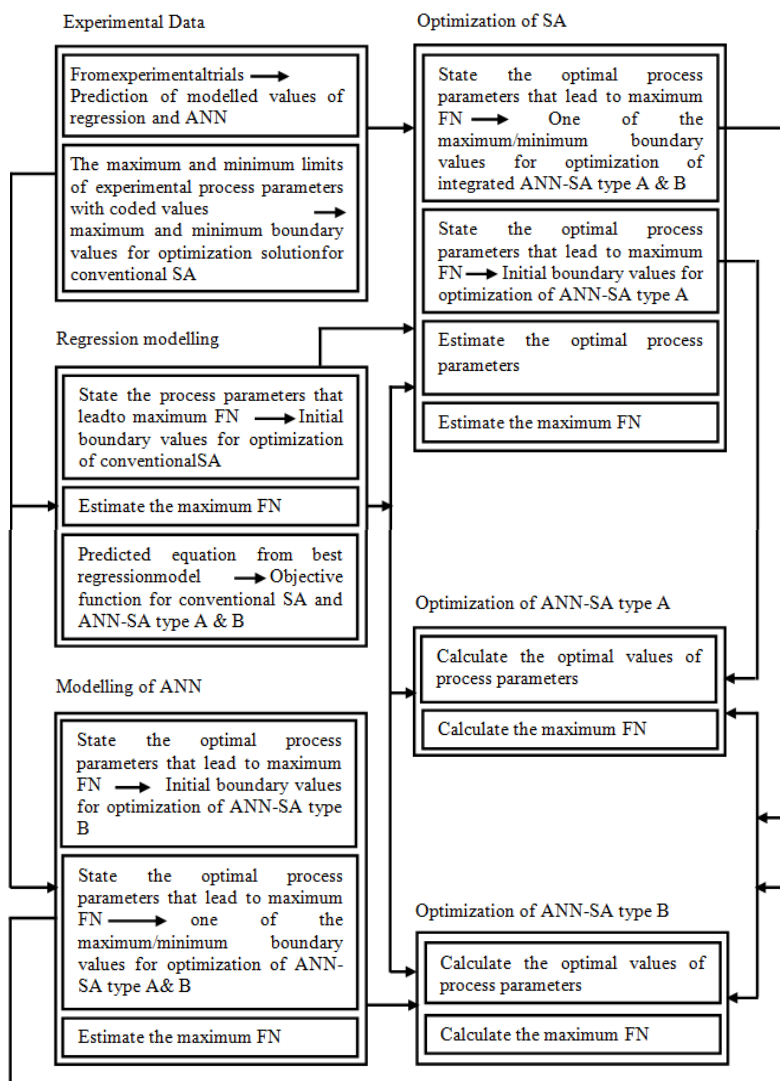


Fig. 5: The flow chart for proposed integrated ANN-SA

- The values of optimum process parameters are estimated. For experimental trial, these values should be within the range of maximum and minimum coded values of experimental design.
- The optimum solution of process parameters with minimum iteration is estimated and compared with other types of optimization for the same optimum process parameters.

The steps followed in integrated ANN-SA type A and integrated ANN-SA type B are satisfied the above three objectives. These are:

- The FN values obtained at different level of combinations of process parameters were used for modeling purpose.
- The mathematical model was developed using multiple regression method. This mathematical model is used to predict the FN.

- From experimental data, the ANN model was developed for predicting maximum FN at non-optimal process parameters.
- The mathematical model developed using regression methods would become the objective function in SA optimization. The maximum and minimum coded values for process parameters of this experiment would define the maximum and minimum value for optimization solution. The initial point for optimization solution is obtained from the process parameters value of regression model and the maximum predicted FN at optimum process parameters was estimated.
- The objective function used in SA optimization is again used in integrated ANN-SA type A. In this optimization, the maximum and minimum boundary values are decided based on the combination of optimum process parameters of SA and ANN models. The optimum process parameters values of SA are fixed as the initial

point of this integration system. Hence, the maximum FN value of the optimization process parameters was estimated.

- The objective function used in integrated ANN-SA optimization is again used in integrated ANN-SA type B. In this optimization, the maximum and minimum boundary values are decided based on the combination of optimum process parameters of SA and ANN models. The process parameters values of the best ANN model are fixed as the initial point for this system. Based on some of the criteria, the maximum FN at optimum process parameters was estimated.

The strategies used for optimization in this study are illustrated in Fig. 5.

Development of mathematical models: The response function representing FN, which can be expressed using Eq. (2):

$$Y = f(A_1, A_2, A_3, A_4) \quad (2)$$

where, Y is response (FN), A_1 is welding current (I) in Ampere, A_2 is welding Speed (S) in cm/min, A_3 is contact tip-to-work piece distance (N) in mm and A_4 is gun angle (T) in degrees. The second order response surface models (Montgomery, 2003) were developed for the four selected parameters. These are given in the Eq. (3) and (4):

$$Y = \beta_0 + \sum_{i=1}^4 \beta_i A_i + \sum_{i=1}^4 \beta_{ii} A_i^2 + \sum_{i < j}^4 \beta_{ij} A_i A_j \quad (3)$$

The Eq. (3) can be written in the form of second order response surface model:

$$Y = \beta_0 + \beta_1 I + \beta_2 S + \beta_3 N + \beta_4 T + \beta_{11} I^2 + \beta_{22} S^2 + \beta_{33} N^2 + \beta_{44} T^2 + \beta_{12} IS + \beta_{13} IN + \beta_{14} IT + \beta_{23} SN + \beta_{24} ST + \beta_{34} NT \quad (4)$$

where, β_0 is free term of the regression equation, the coefficient $\beta_1, \beta_2, \beta_3$ and β_4 are linear terms, the coefficients $\beta_{11}, \beta_{22}, \beta_{33}, \beta_{44}$ are quadratic terms and the coefficients $\beta_{12}, \beta_{13}, \beta_{14}, \beta_{23}, \beta_{24}$ and β_{34} are interaction terms. The coefficients were calculated using QA six sigma-DOE software. After determining the coefficients, the mathematical model of Eq. (5) was developed as follows:

$$\text{Measured FN} = 34.521 - 4.042 I - 4.458 S + 1.542 N - 2.458 T + 0.706 I^2 - 1.669 S^2 - 1.169 T^2 + 0.812 IN + 1.062 IT - 2.938ST \quad (5)$$

To get final mathematical models, the insignificant coefficients were eliminated without affecting the accuracy of the models developed by using t-test. This

Table 4: Predicted ferrite number of regression and ANN (after heat treatment)

Trial No.	Process parameters				Ferrite number	
	I (A)	S (cm/min)	N (mm)	T (degree)	Regression	ANN
02	-1	-1	-1	-1	34.585	28.918
04	1	-1	-1	-1	28.207	27.784
06	-1	1	-1	-1	39.293	35.476
08	1	1	-1	-1	32.915	27.318
10	-1	-1	1	-1	35.331	33.330
12	1	-1	1	-1	17.201	16.994
14	-1	1	1	-1	40.039	33.447
16	1	1	1	-1	21.909	30.001
18	-1	-1	-1	1	29.261	29.023
20	1	-1	-1	1	18.929	20.540
22	-1	1	-1	1	37.605	41.020
24	1	1	-1	1	24.929	22.784
26	-1	-1	1	1	34.521	28.403
28	1	-1	1	1	34.521	35.975
30	-1	1	1	1	34.521	40.265

is done by back elimination technique. The Eq. (6) is the final mathematical model with process parameter in coded form:

$$\text{Measured FN} = 34.521 - 4.042 I - 4.458 S + 1.542 N - 2.458 T + 0.706 I^2 - 1.669 S^2 - 1.169 T^2 + 0.812 IN + 1.062IT - 2.938ST \quad (6)$$

Subsequently, Eq. (6) will be proposed as the objective function for optimization solution of the SA, ANN-SA type A and ANN-SA type B. The results of prediction of the regression model are given in Table 4.

ANN modeling: The common classical method of optimization usually fails to find the optimum solution. Therefore, heuristic algorithms are powerful optimization techniques, which are widely used for solving the complicated problems. The heuristic algorithms, such as Genetic Algorithm (GA), Simulated Annealing (SA), Particle Swam Optimization (PSO) and Ant Colony Optimization (ACO) are generally used. Such optimization techniques have been applied to define the best output parameters through developing mathematical models to specify the relationship between the input process parameters and FN. Mathematical models used to predict FN in duplex stainless steel cladding is important in order to obtain better surface properties. From previous literatures the reader can understand the details about cladding characteristics such as bead height, penetration, dilution have been studied by researchers in different modeling approaches (Nagesh and Datta, 2002, 2010; Kim *et al.*, 2002a, b; Ping *et al.*, 1997; Palani and Murugan, 2007; Parikshit and Dilip, 2007; Yoganandh *et al.*, 2012; Kannan and Murugan, 2005; Murugan and Palani, 2004; Vidyut *et al.*, 2009). There is very limited number of studies that dealt with the applications of ANN (Vitek *et al.*, 2000; Vasudevan *et al.*, 2003). SA to optimize the FN in duplex stainless steel cladding process. Artificial Neural Network (ANN) is one of the powerful tools, which is used for modeling purpose in many fields even if the data relationship is unknown.

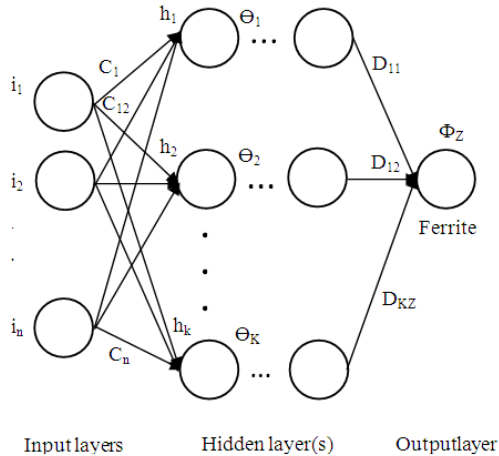


Fig. 6: Configuration of ANN structure with layers and nodes

The objective of this study is to maximize the FN in duplex stainless steel cladding surface. Firstly, ANN was used to model process parameters to set best possible out puts and secondly, simulated annealing was applied to identify those output values with maximum FN. To estimate the FN, an ANN model was developed, which is shown in Fig. 6. In this study, the ANN network structure has two hidden layers each 4 and 2 nodes for estimating the predicted FN. The net input to k in the hidden layer is expressed in Eq. (7):

$$\text{Net_hidden} = \sum C_{j,k} i_j + \Theta_k \tag{7}$$

where is the weight of the input neurons and hidden neurons, i_j is the value of the input which consists of welding current, speed, contact tip-to-work piece distance and gun angle of the experimental sample and Θ_k is the bias of the hidden nodes. From Fig. 6 the net input to unit z the output layer is expressed in Eq. (8):

$$\text{Net_output} = \sum D_{k,z} h_k + \Phi_z \tag{8}$$

where is the weight between hidden and output neurons is the value of the output for the hidden nodes and Φ_z is the bias of the output nodes. From the Eq. (7) and (8), the output for the hidden nodes can give as in Eq. (9) and the output for the output nodes can be given in Eq. (10):

$$h_k = f(\text{net hidden}) \tag{9}$$

$$\Phi_z = f(\text{net output}) = \text{FN} \tag{10}$$

where, f-is the transfer function to predict the value of FN. In order to give better solution in ANN modeling, the number of layers, nodes and testing data are used as trial and error method. At present using integrated methods for optimization solution is familiar than single method (Azlan *et al.*, 2011). Here, 15 experimental data were selected to be a testing data in order to provide good prediction. The result of

prediction of FN values in the ANN model for testing data are given in Table 4. From Table 4, the values of optimum process parameters for providing maximum FN value will be proposed to combine with optimal points of SA. These values will be considered as maximum and minimum boundary values for the optimization of ANN-SA type A and ANN-SA type B.

Optimization: Many optimization techniques have been developed to solve optimization problems with different ways. Unfortunately, no single method is available to solve all types of problem in the existing algorithms. Simulated Annealing is a well-known local optimization approach for solving complex combinatorial problems in manufacturing process. The main aim of this optimization is to find a good solution in an adequate amount of time. The concept of Simulated Annealing is based on the physical annealing process in metallurgy (Kirkpatrick *et al.*, 1983). In this process, physical annealing is named as heating and controlled cooling of metal to bring the material structure from an arbitrary initial state to a final state with the minimum amount of energy. During heating, the metal atoms become free from their current position and arrange themselves randomly. The slow cooling process allows the atoms to find highly structured configurations with lower internal energy than in the initial configuration. The concept of physical process used in this study is considered as an analogy, one which makes the solutions of an optimization problem with possible configurations of the atoms. The main objective of this process is to optimize the FN, which is equivalent to the internal energy. The responsibility of simulated annealing is to assign current values at each step to the variables of succeeding nodes. If assigning that value to a variable has an improvement without conflicts, such assignment will be accepted as a new one. The acceptance of new solutions is based on a probability which is calculated by using a parameter called temperature. The probability depends on the difference between the corresponding values of the objective function and the current temperature. The basic idea of SA is to generate a random point for the purpose of avoiding a trapped one and is able to explore globally for more possible solutions. In annealing process, a molten metal with high temperature is slowly cooled until thermal mobility molecules can move freely till to reach solidification stage. If the cooling is slow enough a perfect crystal is formed in which all the atoms are arranged in a low level lattice with minimum energy. As the metal cools, atoms may align in different directions. In this case, the whole regions of atoms should be reversed to escape this state of local optimum. The required energy is available as heat in the metal and it depends on the current temperature of the system, given by the Boltzmann distribution. As the temperature is decreased, great change become more difficult for the system. When the temperature approaches zero, movements become impossible and the state of the atom is frozen. In this way, for the

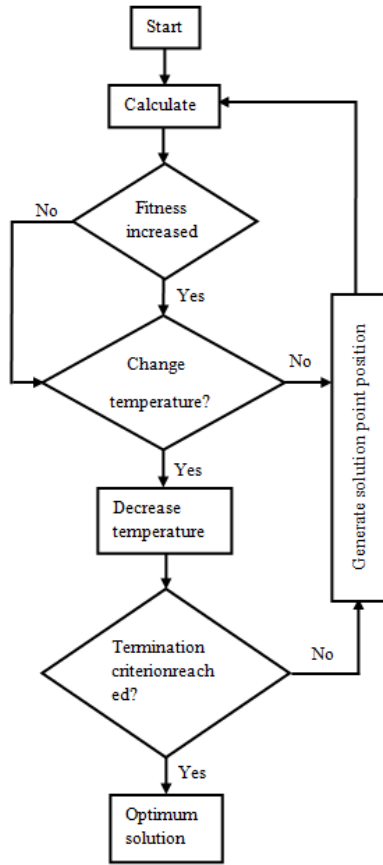


Fig. 7: The flow chart of SA optimization

slowly cooled system, the atoms are arranged in a low energy state and produce a pure crystal. As important part of the SA process is how the inputs are randomized. The randomization process takes the previous values and the current temperature as inputs. The input values are then randomized according to the temperature. A higher will result in more randomization but the lower temperature will result in less randomization. So, there is no specific method defined by the SA algorithm for how to randomize the inputs. The exact nature by which this is done often depends upon the nature of the problem being solved. Figure 7 illustrates the flow on how the SA technique operates in order to search the optimal solution.

SA optimization solution: The main purpose of this optimization is to determine the optimum values of the process parameters that lead to the maximum FN. The regression Eq. (6) is considered to be the fitness function of the optimization solution and is given below:

$$\text{Measured FN}_{\max} = 34.521 - 4.042 I - 4.458S + 1.542 N - 2.458 T + 0.706 I^2 - 1.669 S^2 - 1.169 T^2 + 0.812 IN + 1.062IT - 2.938 ST \quad (11)$$

Table 5: Conditions to define limitation constraint bound of integrated ANN-SA

Condition	Design	
	Lower limit	Upper limit
$(Opt_{ANN}) > (Opt_{SA})$	Opt_{SA}	Opt_{ANN}
$(Opt_{ANN}) < (Opt_{SA})$	Opt_{ANN}	Opt_{SA}

The maximum FN obtained from fitness function Eq. (11) is considered as boundaries (limitations) of the process parameters. The upper and lower boundary limits of process parameters in Table 2 are used as the limitations for optimization and are given below:

$$200 \leq I \leq 300 \quad (12)$$

$$20 \leq S \leq 60 \quad (13)$$

$$22 \leq N \leq 30 \quad (14)$$

$$70 \leq T \leq 90 \quad (15)$$

The process parameters that lead to the maximum FN of the regression model as given in Table 5 will be chosen to be the initial points for the SA solution and are given as follows:

$$\text{Initial point of } I = 225 \quad (16)$$

$$\text{Initial point of } S = 50 \quad (17)$$

$$\text{Initial point of } N = 28 \quad (18)$$

$$\text{Initial point of } T = 75 \quad (19)$$

The limitations of process parameters for the Eq. (12)-(15), the initial points for the Eq. (16)-(19) are obtained using the fitness function Eq. (11). MATLAB tool box is used to find the maximum FN value at the optimum point. The Fig. 8 and 9 show the evidence of results obtained from MATLAB toolbox. From Fig. 8 and 9, the maximum FN value obtained was 49.10. The values of process parameters that lead to maximum FN are 200.21 A, 34.55 cm/min, 22.56 mm and 76.13°. The optimum solution was obtained at 103-th iterations in the SA optimization.

Optimization of integrated ANN-SA:

Type A: As mentioned in above section and Fig. 5, the limits of upper and lower values are obtained from the combination of optimum process parameters of SA and ANN model. These limits are considered as boundary values in ANN-SA type A to get optimum solution. From Table 4, the optimum process parameters values that produce the maximum predicted FN values of the ANN model are 225 A, 50 cm/min, 24 mm and 85° for welding current, welding speed, distance between contact tip-to-specimen and gun angle, respectively.

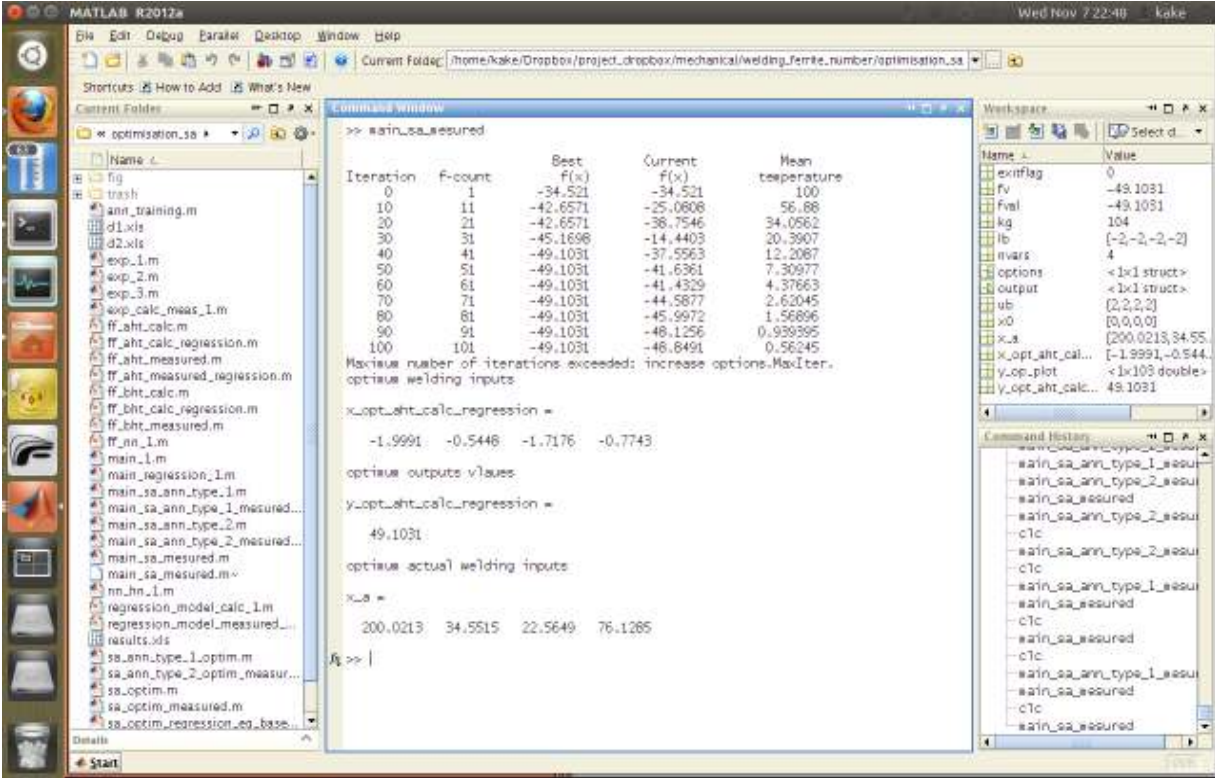


Fig. 8: Optimal solution of SA

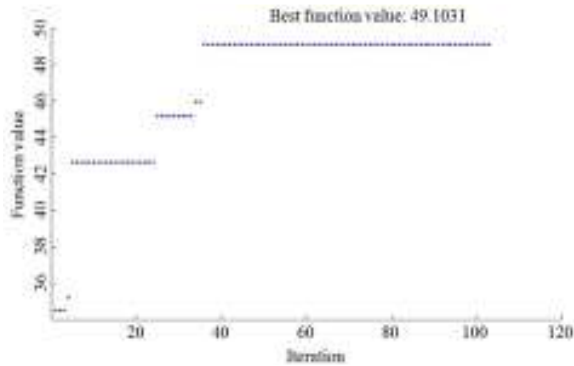


Fig. 9: Fitness function plot of SA

Similarly, from Fig. 8, the values of optimum process parameter of SA are 200.21 A, 34.55 cm/min, 22.56 mm and 76.13°. The conditions stated in Table 5 are used to form the Eq. (20)-(23) with above said values:

$$200.21 \leq I \leq 225 \quad (20)$$

$$34.55 \leq S \leq 50 \quad (21)$$

$$22.56 \leq N \leq 24 \quad (22)$$

$$76.13 \leq T \leq 85 \quad (23)$$

As mentioned in above section and Fig. 5, the initial setting points of ANN-SA type A System is

selected by comparing the values of optimum process parameters that lead to maximum FN in SA and optimum process parameters of ANN with the help of conditions stated in Table 5:

$$\text{Initial point of } I = 200.21 \quad (24)$$

$$\text{Initial point of } S = 34.55 \quad (25)$$

$$\text{Initial point of } N = 22.56 \quad (26)$$

$$\text{Initial point of } T = 76.13 \quad (27)$$

The results of ANN-SA type A is obtained by using the fitness function Eq. (11), the Eq. (20)-(23) and (24)-(27) with same setting process parameters applied in SA and MATLAB toolbox are utilized. The optimum solution of process parameters of ANN-SA Type A are shown in Fig. 10 and 11. From Fig. 10 and 11 the maximum FN value obtained was 52.49. The values of process parameters that lead to maximum FN are 202.42 A, 36.86 cm/min, 27.45 mm and 71.94° and the optimum solution was obtained at 103-th iterations.

Optimization of integrated ANN-SA:

Type B: As mentioned in above section and Fig. 5, similar to integrated ANN-SA type A approach, the fitness function Eq. (11), the boundaries for upper and lower values used for optimization in Eq. (12)-(15)

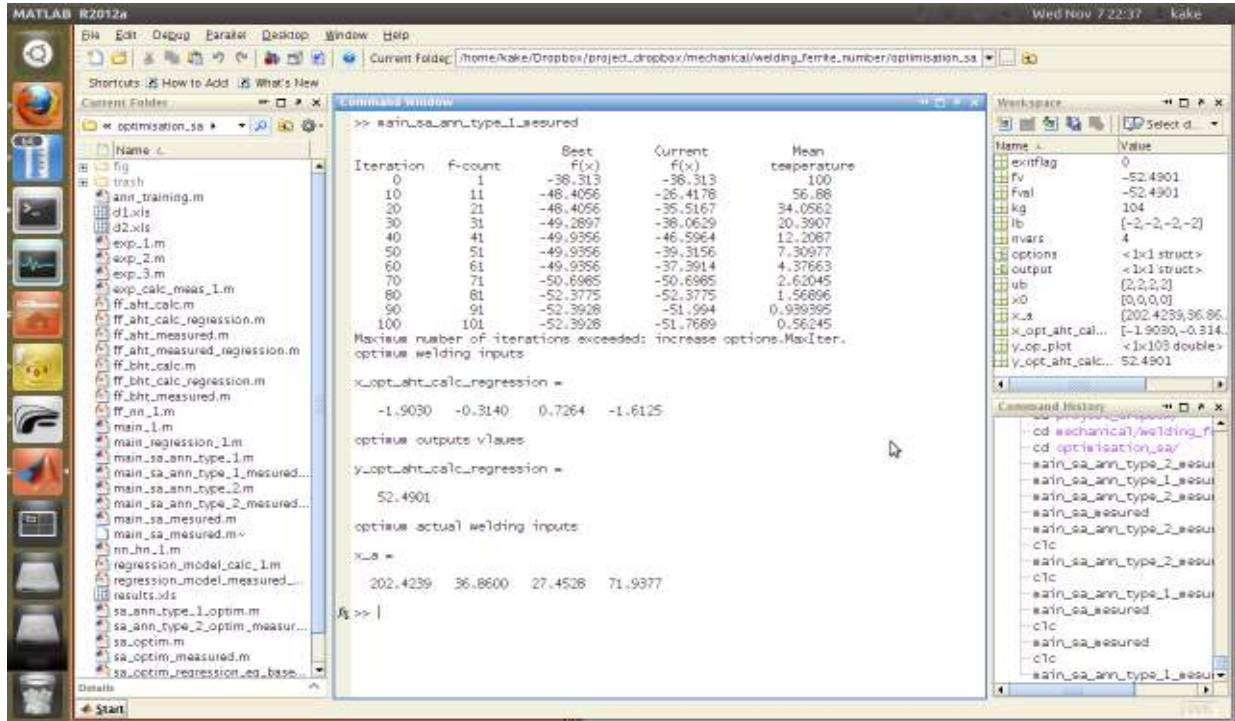


Fig. 10: Optimal solution of integrated ANN-SA type A

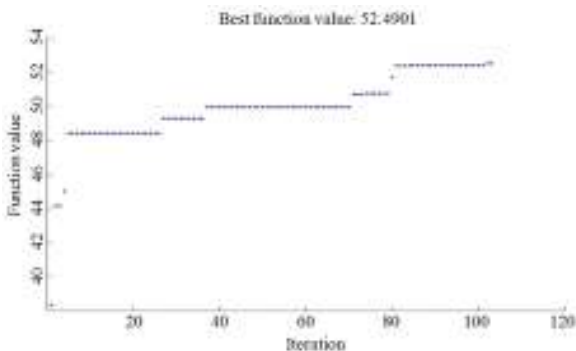


Fig. 11: Fitness function plot of integrated ANN-SA type A

and the points at which the maximum FN value achieved in ANN model will be considered as initial points of ANN-SA type B system. Hence, the Eq. from (28)-(31) are formed using Table 5 as below:

$$\text{Initial point of } I = 225 \quad (28)$$

$$\text{Initial point of } S = 50 \quad (29)$$

$$\text{Initial point of } N = 24 \quad (30)$$

$$\text{Initial point of } T = 85 \quad (31)$$

The Fig. 12 and 13 are showing the results of integrated ANN-SA type B by using MATLAB optimization toolbox. From Fig. 12 and 13, the maximum FN value obtained was 53.98. The values of

process parameters that lead to the maximum FN are 200.05 A, 44.98 cm/min, 25.04 mm and 70.15°. The optimum solution was obtained at 103-the iterations.

RESULTS AND DISCUSSION

Evaluation of the maximum FN value: From Fig. 13, it shows that the maximum FN Value (measured) is 53.98. The maximum FN value obtained in ANN-SA type B is higher, when compared to the result of experimental data, regression model ANN model.

Experimental data vs. integrated ANN-SA: From Table 3, the maximum measured FN value among 31 trials is 49. The maximum FN value obtained from ANN-SA type B is 53.98. Compared to experimental data, the maximum FN value reached in ANN-SA type B is higher value. Consequently, ANN-SA type B is increased the FN value at about 4.98 (10.16%).

Regression vs. integrated ANN-SA: As shown in Table 4, the maximum predicted FN value from regression equation is 40.039. The maximum FN value obtained from ANN-SA type B is 53.98. Compared to regression model, the maximum FN value reached in ANN-SA type B is higher value. Consequently, ANN-SA type B is increased the FN value at about 13.94 (34.81%).

ANN vs. integrated ANN-SA: As shown in Table 4, the maximum FN value (Measured) in ANN model is

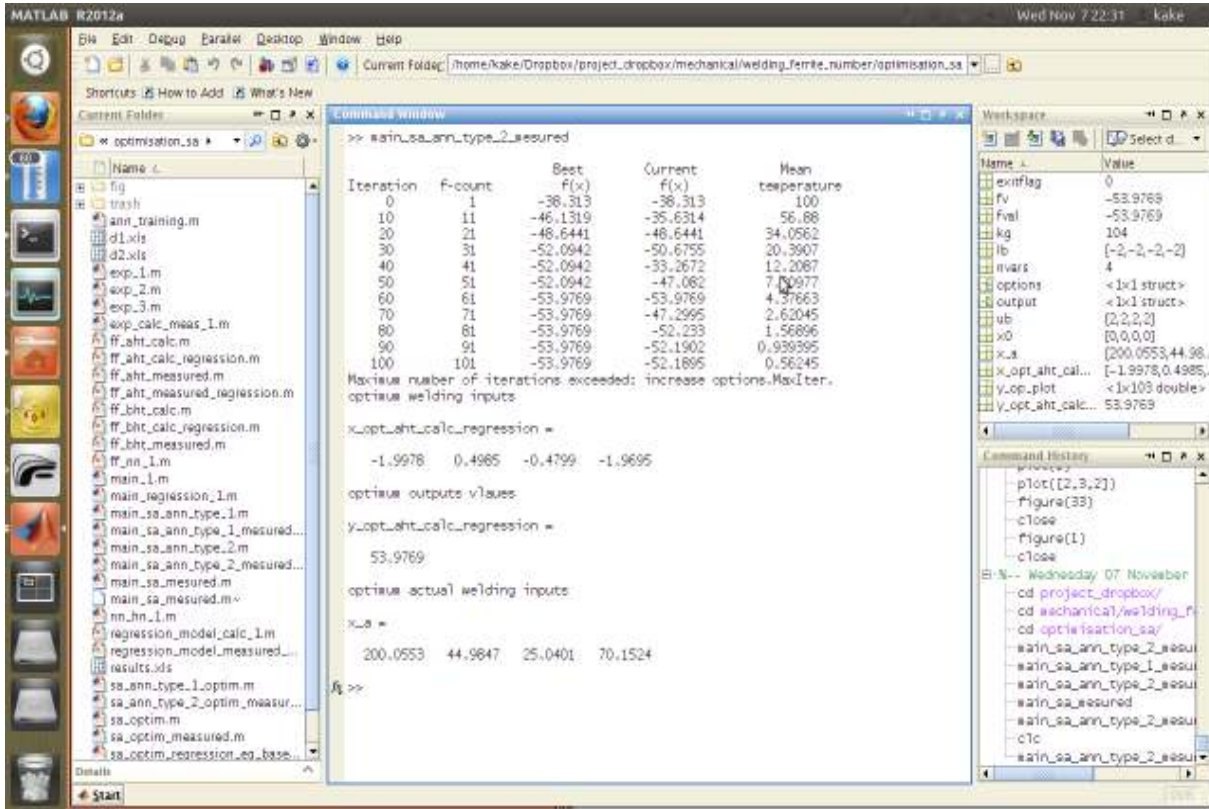


Fig. 12: Optimal solution of integrated ANN-SA type B

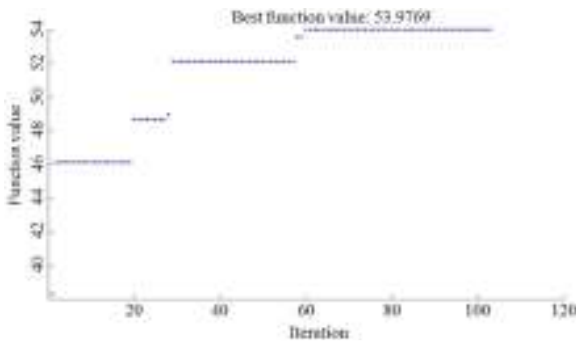


Fig. 13: Fitness function plot of ANN-SA type B

Table 6: Summary of the results

Type of approach	Measured FN value	Optimum points of process parameters	No. of iterations
Regression	40.03	225, 50, 28, 75	-
ANN	41.02	225, 50, 24, 85	-
SA	49.10	200.21, 34.55, 22.56, 76.13	103
ANN-SA type A	52.49	202.42, 36.86, 27.45, 71.94	103
ANN-SA type B	53.97	200.05, 44.98, 25.04, 70.15	103

41.0208. The maximum FN value obtained from ANN-SA type B is 53.98. Compared to ANN model the maximum FN value reached in ANN-SA type B is higher value. Consequently, ANN-SA type B is increased the FN value at about 12.95 (31.59%).

SA vs. integrated ANN-SA: As shown in Fig. 13, FN value was 53.98. As compared to SA optimization Fig. 13 has given maximum FN value. Therefore, the integrated system ANN-SA type B has increased the FN value at about 4.88 (9.94%).

Evaluation of the optimum process:

Parameters: The ranges mentioned against the process parameters in Table 2, are 200-300 A for welding current, 20-60 cm/mm for welding speed, 22-30 mm for contact tip-to-specimen distance, 70-90° for gun angle. The values of optimum process parameters of ANN-SA type B are 200.06 A for welding current, 44.98 cm/mm for welding speed, 25.04 mm for contact tip-to-specimen distance, 70.15° for gun angle. The values of optimum process parameters are within the range of minimum and maximum values of experimental design.

Evaluation of the number of iteration: From Fig. 9, 11 and 13 the number of iterations required to achieve maximum FN in SA, ANN-SA type A and ANN-SA type B are 103. But the FN achieved in SA, ANN-SA type A and ANN-SA type B is 49.10, 52.49 and 53.98, respectively.

CONCLUSION

In this study, integrated ANN-SA type A and ANN-SA type B are proposed to estimate the optimal

solution of process parameters that lead to the maximum FN. The overall results of the duplex stainless steel cladding for four process parameters are summarized in Table 6. The integration of ANN-SA type B has been the effective technique for estimating the maximum FN compared to the experimental, regression and ANN results. The optimum value of process parameters obtained through integrated system has satisfied within the range of maximum and minimum coded values for process parameters of experimental design. As far as the iteration is concerned, different FN have received with same number of iterations. Compared to SA single based optimization, ANN-SA type B system has given better results.

ACKNOWLEDGMENT

The authors wish to express their sincere thanks to M/S Bohler welding, Austria, for providing flux cored duplex stainless steel welding wire for this cladding work. The authors also wish to thank M/S Best Heat Treatment (BHT) and Coimbatore Institute of Technology for their support in arranging and assisting all facilities to carry out this research study.

REFERENCES

- Azlan, M.Z., H. Habibollah and S. Safian, 2011. Estimation of the minimum Machining performance in the abrasive water jet machining using integrated ANN-SA. *Expert Syst. Appl.*, 38(7): 8316-8326.
- Badji, R., B. Belkessa, H. Maza, M. Bouabdallah, B. Bacroix and C. Kahloun, 2004. Effect of post weld heat treatment on microstructure and mechanical properties of welded 2205 duplex stainless steel. *Mater. Sci. Forum.*, 467: 217-222.
- Badji, R. M. Bouabdallah, B. Bacroix, C. Kahloun, B. Belkessa and H. Maza, 2008. Phase transformation and mechanical behavior in annealed 2205 duplex stainless steel welds. *Mater. Charact.*, 59(4): 447-453.
- Cochran, W.G. and G.M. Cox, 1987. *Experimental Designs*. John Wiley and Sons, NY, pp: 370.
- Heejoon, H. and P. Yongsoo, 2009. Effects of heat treatment on the phase ratio and corrosion resistance of duplex stainless steel. *Mater. Trans.*, 50: 1548-1552.
- Kannan, T. and Dr. N. Murugan, 2005. Optimization of FCAW process parameters in duplex stainless steel weld cladding. *Manuf. Technol. Today*, 4(4): 3-7.
- Karlsson, L., 1999. Intermetallic phase precipitation in duplex stainless steels and weld metals: Metallurgy, influence on properties and welding aspects. *Weld. World*, 43(5): 20-41.
- Karlsson, L., L. Ryen and S. Pak, 1995. Precipitation of intermetallic phase in 22% Cr duplex stainless steel weld metals. *Weld. J.*, 74: 28s-40s.
- Kim, D., S. Rhee and H. Park, 2002. Modelling and optimization of a GMAW welding process by genetic algorithm and response surface methodology. *Int. J. Prod. Res.*, 40(7): 1699-1711.
- Kim, I.S., J.S. Son, C.E. Park, C.W. Lee and Y.K.D.V. Prasad, 2002. A study on Prediction of weld bead Height in robotic arc welding using a neural network. *J. Mater. Process. Tech.*, 130: 229-234.
- Kirkpatrick, F., C.D. Gelatt Jr. and M.P. Vecchi, 1983. Optimization by simulated annealing. *Science*, 220(4598): 671-780.
- Kotecki, D.J., 1989. Heat treatment of duplex stainless steel weld metals. *Weld. J.*, 1989: 431s-440s.
- Kotecki, D.J., 1997. Ferrite determination in stainless steel welds: Advances since 1974. *Weld. J.*, 76(1): 24-s-36s.
- Lai, J.K.L., K.W. Wong and D.J. Li, 1995. Effect of solution treatment on the transformation behavior of cold-rolled duplex stainless steels. *Mater. Sci. Eng.*, 203: 356-364.
- Montgomery, D.C., 2003. *Design and Analysis of Experiments*. 5th Edn., John Wiley and Sons, India, pp: 429.
- Murugan, N. and R.S. Parmer, 1994. Effects of MIG process parameters on the geometry of the bead in the automatic surfacing of stainless steel. *J. Mater. Process. Tech.*, 41: 381-398.
- Murugan, N. and P.K. Palani, 2004. Optimization of bead geometry in automatic stainless steel cladding by MIG welding using a Genetic Algorithm. *J. Inst. Eng.*, 84: 49-54.
- Nagesh, D.S. and G.L. Datta, 2002. Prediction of weld bead geometry and penetration in shielded metal arc welding using artificial neural network. *J. Mater. Process. Tech.*, 123: 303-312.
- Nagesh, D.S. and G.L. Datta, 2010. Genetic algorithm for optimization of welding variables for height to width ratio and application of ANN for prediction of bead geometry for TIG welding process. *Appl. Soft Comput.*, 10: 897-907.
- Palani, P.K. and N. Murugan, 2007. Optimization of weld bead geometry for stainless steel cladding deposited by FCAW. *J. Mater. Process. Tech.*, 190: 291-299.
- Parikshit, D. and K.P. Dilip, 2007. Modeling of TIG welding process using conventional regression analysis and neural network-based approaches. *J. Mater. Process. Tech.*, 184: 56-68.
- Ping, L., M.T.C. Fang and J. Lucas, 1997. Modeling of submerged arc weld beads using self-adaptive offset neural networks. *J. Mater. Process. Tech.*, 71: 288-298.

- Vasudevan, M., A.K. Bhaduri, R. Baldev and K. Prasad Rao, 2003. Delta ferrite prediction in stainless steel welds using neural network analysis and comparison with other prediction methods. *J. Mater. Process. Tech.*, 142: 20-28.
- Vidyut, D., K.P. Dilip, G.L. Datta, M.N. Jha, T.K. Saha and A.V. Bapat, 2009. Optimization of bead geometry in electron beam welding using a genetic algorithm. *J. Mater. Process. Tech.*, 209(3): 1151-1157.
- Vitek, J.M., Y.S. Iskander and E.M. Oblow, 2000. Improved ferrite number prediction in stainless steel arc welds using artificial neural network: Part 2: Neural network results. *Weld. Res. Suppl.*, 79(2): 41s-49.
- Yoganandh, J., T. Kannan, S.P. Kumaresh Babu and S. Natarajan, 2012. Optimization of GMAW process parameters in Austenitic stainless steel cladding using Genetic algorithm based computational models. *Exp. Techniques*, 37(5): 48-58.